Optimal antiferromagnets for light dark matter detection

Angelo Esposito[1,2,3,*] and Shashin Pavaskar[4,†]

[1]*Dipartimento di Fisica, Sapienza Università di Roma, Piazzale Aldo Moro 2, I-00185 Rome, Italy*
[2]*INFN Sezione di Roma, Piazzale Aldo Moro 2, I-00185 Rome, Italy*
[3]*School of Natural Sciences, Institute for Advanced Study, Princeton, New Jersey 08540, USA*
[4]*Department of Physics, Carnegie Mellon University, Pittsburgh, Pennsylvania 15213, USA*

We propose antiferromagnets as optimal targets to hunt for sub-MeV dark matter with spin-dependent interactions. These materials allow for multimagnon emission even for very small momentum transfers and are therefore sensitive to dark matter particles as light as the keV. We use an effective theory to compute the event rates in a simple way. Among the materials studied here, we identify nickel oxide (a well-assessed antiferromagnet) as an ideal candidate target. Indeed, the propagation speed of its gapless magnons is very close to the typical dark matter velocity, allowing the absorption of all its kinetic energy, even through the emission of just a single magnon.

I. INTRODUCTION

There is today overwhelming evidence that most of the matter in the Universe is dark. Despite that, the question about its nature arguably remains among the biggest ones in fundamental physics. In particular, the possible dark matter mass spans a range of several orders of magnitude. In light of stringent constraints on heavy weakly interacting massive particles (WIMPs) [1–6], recent years have witnessed an increasing interest in models for sub-GeV dark matter [7–18], also motivating new detection ideas. In particular, dark matter candidates in the keV to GeV range, while still heavy enough to be considered as particles, cannot release appreciable energy via standard nuclear recoil. They therefore require detectors with low-energy thresholds, such as semiconductors [19–26], superconductors [27–31], Dirac materials [32–34], lower-dimensional materials [35–38], and so on (see also Refs. [39–41]).

Among these, the proposals based on superfluid ^{4}He [42–54] and solid crystals [55–59] aim at detecting the collective excitations (phonons) produced by the spin-*independent* interaction of dark matter with the nuclei in the material—for an overview, see Refs. [60–62]. These collective modes have typical energies below $\mathcal{O}(100\text{ meV})$ and are therefore sensitive to particles as light as $m_\chi \sim \mathcal{O}(\text{keV})$.

Different proposals for the detection of single phonons have been recently put forth [63–66].

The targets above are, however, not the most suitable ones to probe possible scenarios where spin-*dependent* interactions of dark matter with the Standard Model are dominant over the spin-independent ones. In this regard, it has been proposed to use ferromagnets [67–69], i.e., materials that exhibit a nonzero macroscopic magnetization in their ground state [70]. The dark matter can interact with the individual spins in the target, exciting their local precession: a propagating collective mode called magnon. The proposals to detect single magnons involve either calorimetric readout [67], using transition edge sensors or microwave kinetic inductance devices, or quantum sensors, which instead couple the magnon mode to a superconducting qubit [72–74]. A generic ferromagnet features several magnon types (branches). However, for sufficiently light dark matter ($m_\chi \lesssim 10$ MeV, for the typical material [67]), the momentum transfer becomes smaller than the inverse separation between the spins. In this regime, the event rate is dominated by the emission of gapless magnons, which, for ferromagnets, are characterized by a quadratic dispersion relation, $\omega(q) = q^2/(2m_\theta)$, with m_θ a mass scale set by the properties of the material under consideration. Moreover, as we argue below, conservation of total magnetization implies that, when only gapless magnons are allowed, no more than one can be produced in each event. Thus, for $m_\chi \lesssim 10$ MeV, the maximum energy that can be released to a ferromagnet is $\omega_{\max} = 4T_\chi x/(1+x)^2$, with T_χ the dark matter kinetic energy and $x \equiv m_\theta/m_\chi$. Typically, $m_\theta \sim \mathcal{O}(\text{MeV})$ (e.g., $m_\theta \simeq 3.5$ MeV for $Y_3Fe_5O_{12}$ [67]; see also Refs. [75,76]), and a sub-MeV dark matter will not deposit all its energy to the target.

*angelo.esposito@uniroma1.it
†spavaska@andrew.cmu.edu

In this work, we show that, instead, *antiferromagnets* are optimal materials to probe the spin-dependent interactions of light dark matter. Similarly to ferromagnets, they also exhibit magnetic order in the ground state, but the spins are antialigned, leading to a vanishing macroscopic magnetization. This leads to two crucial differences: 1) gapless magnons have a linear dispersion relation, $\omega(q) = v_\theta q$, and 2) the interaction with the dark matter can excite any number of them. If only one magnon is emitted, the maximum energy that can be transferred to the antiferromagnet is $\omega_{1,\max} = 4T_\chi y(1 - y)$, with $y \equiv v_\theta/v_\chi$. One of the antiferromagnets we consider here, nickel oxide, features magnons with a propagation speed surprisingly close to the typical dark matter velocity, which allows it to absorb most of the kinetic energy even through a single magnon mode. This is a well-known and well-studied material, which makes it a particularly ideal target. Moreover, the possibility of exciting several magnons in a single event relaxes the kinematic constraints above, allowing any antiferromagnet to absorb the totality of the dark matter kinetic energy, hence being sensitive to masses down to $m_\chi \sim \mathcal{O}(\text{keV})$.

In what follows, we describe antiferromagnets and their interaction with dark matter via an effective field theory (EFT) [71,77,78]. This elucidates the role played by conservation laws in allowing multimagnon emission and allows the computation of the corresponding event rates in a simple way, bypassing the difficulties encountered with more traditional methods (Refs. [79–81]).

We work in natural units, $\hbar = c = 1$, and employ the indices $i, j, k = 1, 2, 3$ for spatial coordinates and $a, b = 1, 2$ for the broken $SO(3)$ generators.

II. EFT

A. Magnons alone

One can often picture an atom in a magnetic material as having a net spin coming from the angular momentum of the electrons localized around it. The Coulomb interaction between electrons pertaining to different atoms induces a coupling between different spins, which, in turns, causes magnetic order in the ground state [82]. In an antiferromagnet, these interactions are such that the spins are antialigned along one direction (Fig. 1), which from now on we take as the z axis. One can then define an order parameter, the so-called Néel vector, as $\mathcal{N} \equiv \sum_i (-1)^i \mathcal{S}_i$,
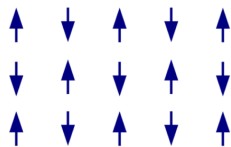

FIG. 1. Schematic representation of the spins in the ground state of an antiferromagnet.

where $\mathcal{S}_i$ is the ith spin and $(-1)^i$ is positive for those sites pointing "up" in the ordered phase and negative for those pointing "down." In the ground state, the Néel vector acquires a nonzero expectation value, $\langle \mathcal{N} \rangle \neq 0$ [77].

In the nonrelativistic limit, a system of three-dimensional spins enjoys an internal $SO(3)$ symmetry. The ground state described above breaks it spontaneously down to only the rotations around the z axis, $SO(3) \to SO(2)$, and the gapless magnons are nothing but the associated Goldstone bosons. As such, at sufficiently low energies, they are described by a universal EFT, very much analogous to the chiral Lagrangian in QCD. A convenient way of parametrizing the magnons is as fluctuations of the order parameter around its equilibrium value, $\hat{n} \equiv e^{i\theta^a S_a} \cdot \hat{z}$, with $a = 1, 2$. Here, $\theta^a(x)$ is the magnon field, and S_a are the broken $SO(3)$ generators.

The EFT Lagrangian is derived purely from symmetry considerations. First of all, one notes that under time reversal each spin changes sign, $\mathcal{S}_i \to -\mathcal{S}_i$. If combined with a translation by one lattice site, which swaps spin up with spin down, this leaves the ground state unchanged. The effective Lagrangian for antiferromagnets must then be invariant under the joint action of these two symmetries. At large distances, translations by one lattice site do not affect the system, and the only requirement is time reversal: the Lagrangian must feature an even number of time derivatives [77]. Moreover, the underlying crystal lattice spontaneously breaks boosts. Assuming, for simplicity, that the material is homogeneous and isotropic at long distances, this implies that there must be explicit invariance under spatial translations and rotations but that space and time derivatives can be treated separately [83]. Since $|\hat{n}| = 1$, the most general low-energy Lagrangian for the gapless magnons [84] in an antiferromagnet is then [71,77],

$$
\begin{aligned}
\mathcal{L}_\theta &= \frac{c_1}{2}(\partial_t \hat{n})^2 - \frac{c_2}{2}(\partial_i \hat{n})^2 \\
&= \frac{c_1}{2}(\dot{\theta}^a)^2 - \frac{c_2}{2}(\partial_i \theta^a)^2 + \cdots,
\end{aligned} \tag{1}
$$

where in the second equality we expanded in small fluctuations around equilibrium. The coefficients $c_{1,2}$ depend on the details of the antiferromagnet under consideration and cannot be determined purely from symmetry.

One recognizes Eq. (1) as the real representation of the Lagrangian of a complex scalar, corresponding to two magnons with linear dispersion relation, $\omega(q) = v_\theta q$, and propagation speed $v_\theta^2 = c_2/c_1$. The two magnons are completely analogous to relativistic particle and antiparticle, and they carry opposite charge under the unbroken $SO(2)$. As shown in Refs. [71,77], the action for a ferromagnet, instead, contains only one time derivative, and it is analogous to that of a nonrelativistic particle, which does not feature excitations with opposite charge. This is the reason why, when coupled to light dark matter, antiferromagnets allow for the emission of more than one

magnon in each event, while ferromagnets do not. We discuss this more in Sec. II B.

As far as our application is concerned, a central role is played by the spin density, which is the time component of the Noether current associated to the original $SO(3)$ symmetry [71,77]. This rotates the $\hat{\bm{n}}$ vector (i.e., $\hat{n}_i \rightarrow R_{ij}\hat{n}_j$), and the current can be computed with standard procedures, giving the spin density:

$$s_i = c_1(\hat{\bm{n}} \times \partial_t \hat{\bm{n}})_i = c_1(\delta_{ia}\dot{\theta}^a + \delta_{i3}\epsilon_{ab}\theta^a\dot{\theta}^b + \cdots). \quad (2)$$

From the equation above, we also deduce that, while the ratio c_2/c_1 can be determined from the magnon speed, the coefficient c_1 can be found from an observable sensitive to the spin density of the antiferromagnet. One such quantity is the neutron scattering cross section (see the Supplemental Material [85] for details).

Finally, our EFT breaks down at short wavelengths, when the dark matter is able to probe the microscopic details of the material. In other words, it loses validity for momenta larger than a certain strong coupling scale, Λ_{UV}. The latter can be estimated, for example, as the momentum for which the dispersion relation sensibly deviates from linearity, which indicates that higher-derivative terms in the Lagrangian (1) become relevant. In this work, we consider three antiferromagnets: nickel oxide (NiO), manganese oxide (MnO), and chromium oxide (Cr_2O_3). In Table I, we report their values of v_θ; c_1; Λ_{UV}; and of their density, ρ_T.

B. Dark matter–magnon interaction

We now study how a dark matter particle couples to the magnon modes introduced in the previous section. To do that, one starts from a specific model for the interaction of dark matter with the Standard Model. This is then computed in the nonrelativistic limit and matched with low-energy quantities, as we now show. For concreteness, we focus on two well-motivated models, which serve as benchmarks to our general point. These were also studied in the context of ferromagnets [67,90]. They are the magnetic dipole (m.d.) and the pseudomediated (p.m.) dark matter, which interact with the Standard Model electron, respectively, as [91–99]

TABLE I. Coefficients for the antiferromagnets considered here. v_θ is taken from the dispersion relation, c_1 is matched from neutron scattering data (see the Supplemental Material [85] for details), and Λ_{UV} is estimated as the momentum for which the dispersion relation deviates from linear by 10%. The densities, ρ_T, are taken from Ref. [86].

	v_θ	c_1 (MeV/Å)	Λ_{UV} (keV)	ρ_T (g/cm³)
NiO [87]	1.3×10^{-4}	0.5	0.6	6.6
MnO [88]	2.5×10^{-5}	4.2	0.5	5.2
Cr_2O_3 [89]	3.5×10^{-5}	0.3	0.9	4.9

$$\mathcal{L}_\chi^{md} = \frac{g_\chi}{\Lambda_\chi} V_{\mu\nu}\bar{\chi}\sigma^{\mu\nu}\chi + g_e V_\mu \bar{e}\gamma^\mu e, \quad (3a)$$

$$\mathcal{L}_\chi^{pm} = g_\chi \phi\bar{\chi}\chi + g_e \phi i\bar{e}\gamma^5 e, \quad (3b)$$

where ϕ and V_μ are ultralight vector and pseudoscalar mediators, χ and e are the dark matter and electron fields, and Λ_χ is a UV scale pertaining to the dark sector. Moreover, $V_{\mu\nu} = \partial_\mu V_\nu - \partial_\nu V_\mu$, and $\sigma^{\mu\nu} = [\gamma^\mu, \gamma^\nu]$. The dipole models can naturally arise in certain technicolor theories, where the DM is a composite particle and can interact with the SM through a vector mediator such as the dark photon [100,101]. Similarly, pseudomediated models can dominate the spin response when the mediator is a pseudo-Goldstone boson [102].

To compute the dark matter–magnon interaction, one can integrate out the mediator and perform the nonrelativistic limit for both the dark matter and electron fields. This can be done either at the level of the matrix elements or integrating out antiparticles, similarly to the Heavy Quark Effective Theory procedure [103]. (See also the Supplemental Material [85] for a quick review). After this, the dark matter–magnon interaction in the two instances is

$$\mathcal{L}_{int}^{md} = -\frac{4g_\chi g_e}{\Lambda_\chi m_e}\left(\chi_{nr}^\dagger \frac{\sigma^i}{2}\chi_{nr}\right)\left(\delta^{ij} - \frac{\nabla^i\nabla^j}{\nabla^2}\right)\left(e_{nr}^\dagger \frac{\sigma^j}{2}e_{nr}\right)$$
$$\xrightarrow{IR} -\frac{4g_\chi g_e}{\Lambda_\chi m_e}\left(\chi_{nr}^\dagger \frac{\sigma^i}{2}\chi_{nr}\right)\left(\delta^{ij} - \frac{\nabla^i\nabla^j}{\nabla^2}\right)s^j, \quad (4a)$$

$$\mathcal{L}_{int}^{pm} = -\frac{g_\chi g_e}{m_e}\chi_{nr}^\dagger\chi_{nr}\nabla^{-2}\bm{\nabla} \cdot \left(e_{nr}^\dagger \frac{\bm{\sigma}}{2}e_{nr}\right)$$
$$\xrightarrow{IR} -\frac{g_\chi g_e}{m_e}\chi_{nr}^\dagger\chi_{nr}\nabla^{-2}\bm{\nabla} \cdot \bm{s}, \quad (4b)$$

where χ_{nr} and e_{nr} are nonrelativistic fields and $\bm{\sigma}$ are Pauli matrices. We also used the fact that $e_{nr}^\dagger\bm{\sigma}e_{nr}/2$ is the electron spin density operator. When running toward low energies, it will remain such, except that it must be expressed in terms of the correct low-energy degrees of freedom: the magnons rather than the single electrons.

One can now understand why antiferromagnets allow for multimagnon emission while ferromagnets do not. As shown in Eqs. (4), dark matter interacts with magnons via the spin density, whose components, $(s_x \pm is_y, s_z)$, have at most charge 1 under the unbroken $SO(2)$. In a ferromagnet, this charge can be carried only by a single magnon mode. In an antiferromagnet, instead, there are two magnon modes carrying opposite charges. Hence, any coupling to the spin density operator will allow multi-magnon emission.

Given the Lagrangians in Eqs. (4) and the spin density in Eq. (2), one derives Feynman rules for the dark matter–magnon interaction, obtaining

$$\begin{array}{c} a, \lambda_1 \\ \vdots \\ s \xrightarrow{\hspace{1.5cm}} s' \end{array} = -\frac{g_\chi g_e \sqrt{c_1}}{m_e}\omega \times \begin{cases} \frac{4}{\Lambda_\chi}P_{ia}(\boldsymbol{q})\sigma^i & \text{md} \\ q^a/q^2 & \text{pm} \end{cases},$$

$$\begin{array}{c} a, \lambda_1 \quad b, \lambda_2 \\ \diagdown \quad \diagup \\ s \xrightarrow{\hspace{1.5cm}} s' \end{array} = \frac{g_\chi g_e}{m_e}(\omega_1 - \omega_2)\epsilon_{ab} \times \begin{cases} \frac{4}{\Lambda_\chi}P_{iz}(\boldsymbol{q})\sigma^i & \text{md} \\ q^z/q^2 & \text{pm} \end{cases}.$$

Solid lines represent a dark matter with polarization $s^{(\prime)}$, and dashed ones represent magnons with momenta $\boldsymbol{q}_{1,2}$, energies $\omega_{1,2}$, polarizations $\lambda_{1,2}$, and carrying an index a, $b = 1, 2$. The total momentum and energy carried by the magnons are $\boldsymbol{q}$ and ω, with $P_{ij}(\boldsymbol{q}) \equiv \delta_{ij} - q_i q_j/q^2$. External dark matter lines come with standard nonrelativistic bispinors, while external magnon lines come with a polarization vector, $\hat{\boldsymbol{\varepsilon}}_\pm = (1, \pm i)/\sqrt{2}$ [71].

With this at hand, one can compute matrix elements for the emission rate of any number of gapless magnons with simple diagrammatic methods, exactly as one would do for relativistic particles. In particular, the matrix element for the emission of *any* number of low-energy magnons is completely fixed by symmetry and by a single effective coefficient, c_1. In a more traditional formulation, the computation of multimagnon scattering is substantially complicated by the failure of the Holstein-Primakoff approach, which mandates for a more involved treatment [81].

III. EVENT RATES

We now have everything we need to compute the expected event rates for the emission of one and two magnons by a dark matter particle. For a target material with density ρ_T, the total event rate per unit target mass can be evaluated by averaging the magnon emission rate over the dark matter velocity distribution, $f(\boldsymbol{v}_\chi + \boldsymbol{v}_e)$:

$$R = \frac{\rho_\chi}{\rho_T m_\chi}\int d^3 v_\chi f(\boldsymbol{v}_\chi + \boldsymbol{v}_e)\Gamma(v_\chi). \tag{5}$$

The local dark matter density is taken to be $\rho_\chi = 0.4\,\text{GeV/cm}^3$ [104]. The velocity distribution in the Milky Way is instead considered as a truncated Maxwellian given by the standard halo model, with dispersion $v_0 = 230\,\text{km/s}$, escape velocity $v_{\text{esc}} = 600\,\text{km/s}$ and boosted with respect to the Galactic rest frame by the Earth velocity, $v_e = 240$ km/s [104,105]. In the following, we present the projected reach for the case of single- and two-magnon emission for the antiferromagnets NiO, MnO, and Cr_2O_3.

A. One magnon

Using the Feynman rules presented in Sec. II B, we compute the rates for the emission of a single gapless magnon. For the two benchmark models, they read

$$\frac{d\Gamma}{d\omega} = \frac{g_\chi^2 g_e^2 c_1}{\pi v_\chi m_e^2} \times \begin{cases} \frac{1+\langle\cos^2\eta\rangle}{2v_\theta^2\Lambda_\chi^2}\omega^2 & \text{md} \\ \frac{\langle\sin^2\eta\rangle}{4} & \text{pm} \end{cases}, \tag{6}$$

where η is the angle between the Néel vector, $\mathcal{N}$, and the magnon momentum, $\boldsymbol{q}$, and $\langle\cdots\rangle$ represents an average over the direction of the latter. The decay rate is then a function of the relative angle between the magnetization and the direction of the incoming dark matter. Moreover, the magnon is emitted at fixed Cherenkov angle with respect to the incoming dark matter, $\cos\theta = q/(2m_\chi v_\chi) + v_\theta/v_\chi$. The final event rate, Eq. (5), depends on the relative angle between $\boldsymbol{v}_e$ and $\mathcal{N}$. This leads to a daily modulation, which can possibly be used for background discrimination. To reduce the computational burden, we fix the two vectors to be parallel (more details can be found in the Supplemental Material [85]).

To obtain the decay rate, one integrates Eq. (6) over magnon energies between $\omega_{\min}$ and $\omega_{\max}$. The first one is set by the detector energy threshold. For the case of calometric readout, the best sensitivities that have been envisioned are of $\mathcal{O}(\text{meV})$ [106]. We thus set $\omega_{\min} = 1$ meV. The maximum magnon energy is instead set by either the cutoff of the EFT or by kinematics. Specifically, $\cos\theta < 1$ limits the possible momentum transfer, implying $\omega_{\max} = \min(v_\theta\Lambda_{\text{UV}}, 2m_\chi v_\theta(v_\chi - v_\theta))$.

Our projected reach for the three target materials are shown in Fig. 2, as compared to the following dark matter–electron cross sections, obtained from the interactions in Eqs. (3) in vacuum evaluated at the reference momentum $q_0 = \alpha m_e$ [67]:

$$\bar{\sigma}_e = \frac{g_\chi^2 g_e^2}{\pi} \times \begin{cases} \frac{1}{\Lambda_\chi^2}\frac{6m_\chi^2+m_e^2}{(m_\chi+m_e)^2} & \text{md} \\ \frac{1}{4\alpha^2 m_e^2}\frac{m_\chi^2}{(m_\chi+m_e)^2} & \text{pm} \end{cases}. \tag{7}$$

Moreover, to avoid white dwarf cooling and self-interacting dark matter constraints, we impose χ to be a 5% subcomponent of dark matter for the pseudomediated model [67]. Following convention, and for a simpler comparison with other proposals, we also assume zero background.

Importantly, NiO is sensitive to masses down to $m_\chi \simeq 5$ keV, even in the single-magnon channel. This, as mentioned in the Introduction, is due to the good matching between the magnon and dark matter velocities. For $m_\chi \gtrsim 1$ MeV, the rate starts receiving contributions from momenta above the cutoff, indicating that gapped magnons, not captured by the EFT, become relevant.

B. Two magnons

We consider now the emission of two magnons of energies and momenta $\omega_{1,2}$ and $\boldsymbol{q}_{1,2}$, and total energy and momentum ω and $\boldsymbol{q}$, by a dark matter of initial and final momentum $\boldsymbol{k}$ and $\boldsymbol{k}'$. Using conservation of energy and momentum, the decay rate can be written as
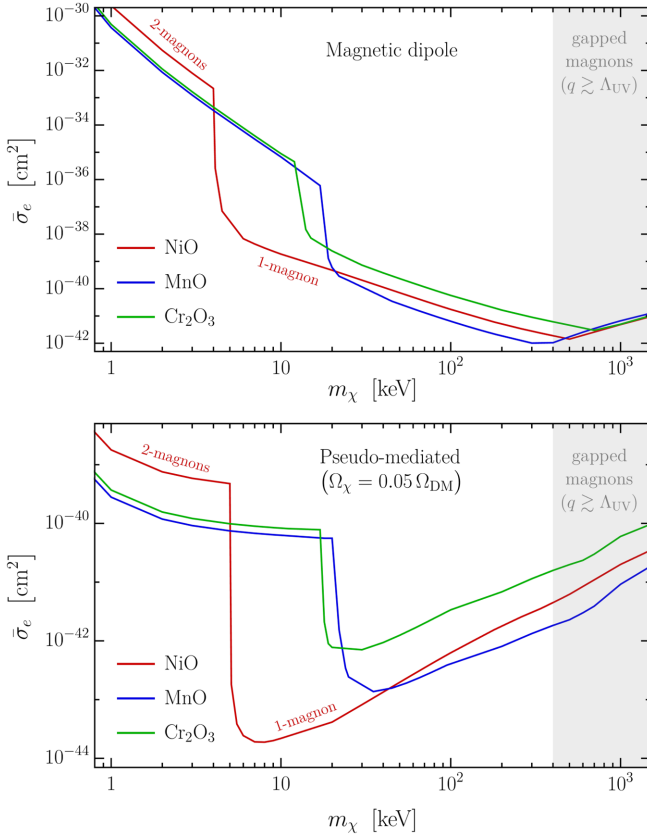
FIG. 2.   Projected reach at 95% C.L. for a kilogram of material and a year of exposure assuming zero background, for the magnetic dipole (upper panel) and pseudomediated (lower panel) models. For the latter, we assume $\Omega_\chi/\Omega_{\mathrm{DM}} = 0.05$. The lowest-mass region is reached via the two-magnon channel. The gray region corresponds to masses for which gapped magnons are expected to play an important role. The magnetization is taken to be parallel to the Earth's velocity.

$$\Gamma = \int \frac{k'^2 dk' d\cos\psi \, dq_1}{4(2\pi)^3 v_\theta^3 q} |\mathcal{M}|^2 = \int \frac{d\omega dq dq_1}{4(2\pi)^3 v_\theta^3 v_\chi} |\mathcal{M}|^2, \quad (8)$$

where ψ denotes the angle between $\boldsymbol{k}$ and $\boldsymbol{k'}$. In the second equality, we also used $k'^2 dk' d\cos\psi = (q/v_\chi)dqd\omega$. Conservation of energy and momentum further implies $q_1 \leq (\omega + v_\theta q)/(2v_\theta)$. Thus, including also the EFT cutoff, the integral above is performed over $\omega_{\min} \leq \omega \leq \min(v_\theta\Lambda_{\mathrm{UV}}, \frac{1}{2}m_\chi v_\chi^2)$, $0 \leq q \leq \min(\Lambda_{\mathrm{UV}}, 2m_\chi v_\chi)$, and $0 \leq q_1 \leq \min(\Lambda_{\mathrm{UV}}, (\omega + v_\theta q)/(2v_\theta))$. Again, we assume ideal calorimetric readout and set $\omega_{\min} = 1$ meV.

The projected reach for the two-magnon case is again shown in Fig. 2. This process allows us to explore an even larger parameter space, by going down to masses as low as

$m_\chi \sim 1$ keV. Because of improved kinematic matching, the mass reach is now almost independent of the target material. For the lightest dark matter, the momentum transfer is much smaller than the energy transfer, and the two magnons are emitted almost back to back, with possible interesting implications for background rejection [50]. Similar to the one-magnon case, the EFT predictions are unreliable for masses above 1 MeV.

IV. CONCLUSION

We have shown how well-assessed antiferromagnets can be used as optimal probes for sub-MeV dark matter with spin-dependent interactions. At low energies, these materials feature gapless magnons with two different polarizations, hence allowing for the emission of an arbitrary number of excitations. This, in turns, extends the potential reach down to $m_\chi \sim \mathcal{O}(\mathrm{keV})$. As compared to ferromagnets [67], they have similar sensitivities on the dark matter couplings, but they probe masses more than an order of magnitude lighter. Interestingly, one of these antiferromagnets, nickel oxide, sustains magnon modes with a propagation speed accidentally close to the typical dark matter velocity, which allows it to absorb most of the dark matter energy already via the (dominant) one-magnon channel. These results complement what has already been proposed for dark matter with spin-independent interactions [43,44,46,55,57], allowing coverage of the same mass region.

Moreover, the introduction of an EFT treatment to the problem opens the possibility of evaluating more involved observables, as, for example, multimagnon events with strong directionality and the potential for background discrimination [50]. Finally, a simple extension of our EFT would allow the description of the magnon-phonon coupling [71]. This could be used to probe both spin-dependent and spin-independent interactions with a single target. Finally, it is interesting to study the prospect of our materials for axion absorption and compare with the proposal in Refs. [68,69,78,107,108] (see also Refs. [109–111]). We leave these and other questions for future work.

[1] R. Agnese *et al.* (SuperCDMS Collaboration), Phys. Rev. Lett. **116**, 071301 (2016).

[2] D. S. Akerib *et al.* (LUX Collaboration), Phys. Rev. Lett. **118**, 021303 (2017).

[3] R. Agnese *et al.* (SuperCDMS Collaboration), Phys. Rev. Lett. **121**, 051301 (2018); **122**, 069901(E) (2019).

[4] E. Aprile *et al.* (XENON Collaboration), Phys. Rev. Lett. **123**, 251801 (2019).

[5] A. H. Abdelhameed *et al.* (CRESST Collaboration), Phys. Rev. D **100**, 102002 (2019).

[6] Q. Wang *et al.* (PandaX-II Collaboration), Chin. Phys. C **44**, 125001 (2020).

[7] C. Boehm, P. Fayet, and J. Silk, Phys. Rev. D **69**, 101302 (2004).

[8] C. Boehm and P. Fayet, Nucl. Phys. **B683**, 219 (2004).

[9] M. J. Strassler and K. M. Zurek, Phys. Lett. B **651**, 374 (2007).

[10] D. Hooper and K. M. Zurek, Phys. Rev. D **77**, 087302 (2008).

[11] J. L. Feng and J. Kumar, Phys. Rev. Lett. **101**, 231301 (2008).

[12] A. Falkowski, J. T. Ruderman, and T. Volansky, J. High Energy Phys. 05 (2011) 106.

[13] T. Lin, H.-B. Yu, and K. M. Zurek, Phys. Rev. D **85**, 063503 (2012).

[14] Y. Hochberg, E. Kuflik, T. Volansky, and J. G. Wacker, Phys. Rev. Lett. **113**, 171301 (2014).

[15] R. T. D'Agnolo and J. T. Ruderman, Phys. Rev. Lett. **115**, 061301 (2015).

[16] E. Kuflik, M. Perelstein, N. R.-L. Lorier, and Y.-D. Tsai, Phys. Rev. Lett. **116**, 221302 (2016).

[17] D. Green and S. Rajendran, J. High Energy Phys. 10 (2017) 013.

[18] R. T. D'Agnolo, C. Mondino, J. T. Ruderman, and P.-J. Wang, J. High Energy Phys. 08 (2018) 079.

[19] R. Essig, J. Mardon, and T. Volansky, Phys. Rev. D **85**, 076007 (2012).

[20] P. W. Graham, D. E. Kaplan, S. Rajendran, and M. T. Walters, Phys. Dark Universe **1**, 32 (2012).

[21] R. Essig, M. Fernandez-Serra, J. Mardon, A. Soto, T. Volansky, and T.-T. Yu, J. High Energy Phys. 05 (2015) 046.

[22] Y. Hochberg, T. Lin, and K. M. Zurek, Phys. Rev. D **95**, 023013 (2017).

[23] I. M. Bloch, R. Essig, K. Tobioka, T. Volansky, and T.-T. Yu, J. High Energy Phys. 06 (2017) 087.

[24] S. Knapen, J. Kozaczuk, and T. Lin, Phys. Rev. Lett. **127**, 081805 (2021).

[25] Z.-L. Liang, C. Mo, F. Zheng, and P. Zhang, Phys. Rev. D **106**, 043004 (2022).

[26] K. V. Berghaus, A. Esposito, R. Essig, and M. Sholapurkar, J. High Energy Phys. 01 (2023) 023.

[27] Y. Hochberg, Y. Zhao, and K. M. Zurek, Phys. Rev. Lett. **116**, 011301 (2016).

[28] Y. Hochberg, T. Lin, and K. M. Zurek, Phys. Rev. D **94**, 015019 (2016).

[29] Y. Hochberg, I. Charaev, S.-W. Nam, V. Verma, M. Colangelo, and K. K. Berggren, Phys. Rev. Lett. **123**, 151802 (2019).

[30] S. M. Griffin, Y. Hochberg, K. Inzani, N. Kurinsky, T. Lin, and T. Chin, Phys. Rev. D **103**, 075002 (2021).

[31] Y. Hochberg, B. V. Lehmann, I. Charaev, J. Chiles, M. Colangelo, S. W. Nam, and K. K. Berggren, Phys. Rev. D **106**, 112005 (2022).

[32] Y. Hochberg, Y. Kahn, M. Lisanti, K. M. Zurek, A. G. Grushin, R. Ilan, S. M. Griffin, Z.-F. Liu, S. F. Weber, and J. B. Neaton, Phys. Rev. D **97**, 015004 (2018).

[33] A. Coskuner, A. Mitridate, A. Olivares, and K. M. Zurek, Phys. Rev. D **103**, 016006 (2021).

[34] R. M. Geilhufe, F. Kahlhoefer, and M. W. Winkler, Phys. Rev. D **101**, 055005 (2020).

[35] L. M. Capparelli, G. Cavoto, D. Mazzilli, and A. D. Polosa, Phys. Dark Universe **9–10**, 24 (2015); **11**, 79(E) (2016).

[36] Y. Hochberg, Y. Kahn, M. Lisanti, C. G. Tully, and K. M. Zurek, Phys. Lett. B **772**, 239 (2017).

[37] G. Cavoto, E. N. M. Cirillo, F. Cocina, J. Ferretti, and A. D. Polosa, Eur. Phys. J. C **76**, 349 (2016).

[38] G. Cavoto, F. Luchetta, and A. D. Polosa, Phys. Lett. B **776**, 338 (2018).

[39] A. Arvanitaki, S. Dimopoulos, and K. Van Tilburg, Phys. Rev. X **8**, 041001 (2018).

[40] P. C. Bunting, G. Gratta, T. Melia, and S. Rajendran, Phys. Rev. D **95**, 095001 (2017).

[41] H. Chen, R. Mahapatra, G. Agnolet, M. Nippe, M. Lu, P. C. Bunting, T. Melia, S. Rajendran, G. Gratta, and J. Long, arXiv:2002.09409.

[42] W. Guo and D. N. McKinsey, Phys. Rev. D **87**, 115001 (2013).

[43] K. Schutz and K. M. Zurek, Phys. Rev. Lett. **117**, 121302 (2016).

[44] S. Knapen, T. Lin, and K. M. Zurek, Phys. Rev. D **95**, 056019 (2017).

[45] S. A. Hertel, A. Biekert, J. Lin, V. Velan, and D. N. McKinsey, Phys. Rev. D **100**, 092007 (2019).

[46] F. Acanfora, A. Esposito, and A. D. Polosa, Eur. Phys. J. C **79**, 549 (2019).

[47] A. Caputo, A. Esposito, and A. D. Polosa, Phys. Rev. D **100**, 116007 (2019).

[48] A. Caputo, A. Esposito, E. Geoffray, A. D. Polosa, and S. Sun, Phys. Lett. B **802**, 135258 (2020).

[49] G. Baym, D. H. Beck, J. P. Filippini, C. J. Pethick, and J. Shelton, Phys. Rev. D **102**, 035014 (2020); **104**, 019901 (E) (2021).

[50] A. Caputo, A. Esposito, F. Piccinini, A. D. Polosa, and G. Rossi, Phys. Rev. D **103**, 055017 (2021).

[51] K. T. Matchev, J. Smolinsky, W. Xue, and Y. You, J. High Energy Phys. 05 (2022) 034.

[52] Y. You, J. Smolinsky, W. Xue, K. T. Matchev, K. Gunther, Y. Lee, and T. Saab, arXiv:2208.14474.

[53] B. von Krosigk *et al.*, in *14th International Workshop on the Identification of Dark Matter 2022* (2022), arXiv:2209.10950.

[54] G. M. Seidel and C. Enss, arXiv:2210.06283.

[55] S. Knapen, T. Lin, M. Pyle, and K. M. Zurek, Phys. Lett. B **785**, 386 (2018).

[56] S. Griffin, S. Knapen, T. Lin, and K. M. Zurek, Phys. Rev. D **98**, 115034 (2018).

[57] B. Campbell-Deem, P. Cox, S. Knapen, T. Lin, and T. Melia, Phys. Rev. D **101**, 036006 (2020); **102**, 019904(E) (2020).

[58] P. Cox, T. Melia, and S. Rajendran, Phys. Rev. D **100**, 055011 (2019).

[59] B. Campbell-Deem, S. Knapen, T. Lin, and E. Villarama, Phys. Rev. D **106**, 036019 (2022).

[60] S. M. Griffin, K. Inzani, T. Trickle, Z. Zhang, and K. M. Zurek, Phys. Rev. D **101**, 055004 (2020).

[61] T. Trickle, Z. Zhang, K. M. Zurek, K. Inzani, and S. M. Griffin, J. High Energy Phys. 03 (2020) 036.

[62] Y. Kahn and T. Lin, Rep. Prog. Phys. **85**, 066901 (2022).

[63] H. J. Maris, G. M. Seidel, and D. Stein, Phys. Rev. Lett. **119**, 181303 (2017).

[64] D. Osterman, H. Maris, G. Seidel, and D. Stein, J. Phys. Conf. Ser. **1468**, 012071 (2020).

[65] S. A. Lyon, K. Castoria, E. Kleinbaum, Z. Qin, A. Persaud, T. Schenkel, and K. Zurek, arXiv:2201.00738.

[66] A. Das, N. Kurinsky, and R. K. Leane, arXiv:2210.09313.

[67] T. Trickle, Z. Zhang, and K. M. Zurek, Phys. Rev. Lett. **124**, 201801 (2020).

[68] A. Mitridate, T. Trickle, Z. Zhang, and K. M. Zurek, Phys. Rev. D **102**, 095005 (2020).

[69] S. Chigusa, T. Moroi, and K. Nakayama, Phys. Rev. D **101**, 096013 (2020).

[70] The materials presented in Refs. [67,68] are actually insulating ferrimagnets. This makes no difference in our discussion [71]. We refer to ferromagnets, which are conceptually simpler.

[71] S. Pavaskar, R. Penco, and I. Z. Rothstein, SciPost Phys. **12**, 155 (2022).

[72] D. Lachance-Quirion, S. P. Wolski, Y. Tabuchi, S. Kono, K. Usami, and Y. Nakamura, Science **367**, 425 (2020).

[73] D. Lachance-Quirion, Y. Tabuchi, A. Gloppe, K. Usami, and Y. Nakamura, Appl. Phys. Express **12**, 070101 (2019).

[74] D. Lachance-Quirion, Y. Tabuchi, S. Ishino, A. Noguchi, T. Ishikawa, R. Yamazaki, and Y. Nakamura, Sci. Adv. **3**, e1603150 (2017).

[75] C. Srivastava and R. Aiyar, J. Phys. C **20**, 1119 (1987).

[76] M. Pajda, J. Kudrnovský, I. Turek, V. Drchal, and P. Bruno, Phys. Rev. B **64**, 174402 (2001).

[77] C. P. Burgess, Phys. Rep. **330**, 193 (2000).

[78] J. Schütte-Engel, D. J. E. Marsh, A. J. Millar, A. Sekine, F. Chadha-Day, S. Hoof, M. N. Ali, K.-C. Fong, E. Hardy, and L. Šmejkal, J. Cosmol. Astropart. Phys. 08 (2021) 066.

[79] G. L. Squires, *Introduction to the Theory of Thermal Neutron Scattering* (Courier Corporation, Chelmsford, MA, 1996).

[80] S. Lovesey, *Theory of Neutron Scattering from Condensed Matter: Nuclear Scattering*, International Series of Monographs on Physics (Clarendon Press, Oxford, UK, 1984).

[81] F. J. Dyson, Phys. Rev. **102**, 1217 (1956).

[82] N. Ashcroft and N. Mermin, *Solid State Physics* (Cengage Learning, Boston, MA, 2011).

[83] We treat the underlying solid as a background, which spontaneously breaks some spacetime symmetries. The corresponding Goldstone bosons, the phonons, realize these symmetries nonlinearly and can be included in the description if necessary [71].

[84] Crystalline anisotropy, which arises from spin-orbit coupling, can result in a small gap for magnons. This is analogous to the pion obtaining a mass due to the explicit breaking of chiral symmetry.

[85] See Supplemental Material at http://link.aps.org/supplemental/10.1103/PhysRevD.108.L011901 for details about the matching procedure, the nonrelativistic limit and the event rate calculation.

[86] A. Jain, S. P. Ong, G. Hautier, W. Chen, W. D. Richards, S. Dacek, S. Cholia, D. Gunter, D. Skinner, G. Ceder, and K. A. Persson, APL Mater. **1**, 011002 (2013).

[87] M. T. Hutchings and E. J. Samuelsen, Solid State Commun. **9**, 1011 (1971).

[88] G. Pepy, J. Phys. Chem. Solids **35**, 433 (1974).

[89] E. Samuelsen, M. Hutchings, and G. Shirane, Solid State Commun. **7**, 1043 (1969).

[90] T. Trickle, Z. Zhang, and K. M. Zurek, Phys. Rev. D **105**, 015001 (2022).

[91] K. Sigurdson, M. Doran, A. Kurylov, R. R. Caldwell, and M. Kamionkowski, Phys. Rev. D **70**, 083501 (2004); **73**, 089903(E) (2006).

[92] E. Masso, S. Mohanty, and S. Rao, Phys. Rev. D **80**, 036009 (2009).

[93] S. Chang, N. Weiner, and I. Yavin, Phys. Rev. D **82**, 125011 (2010).

[94] V. Barger, W.-Y. Keung, and D. Marfatia, Phys. Lett. B **696**, 74 (2011).

[95] A. L. Fitzpatrick, W. Haxton, E. Katz, N. Lubbers, and Y. Xu, J. Cosmol. Astropart. Phys. 02 (2013) 004.

[96] M. I. Gresham and K. M. Zurek, Phys. Rev. D **89**, 123521 (2014).

[97] E. Del Nobile, G. B. Gelmini, P. Gondolo, and J.-H. Huh, J. Cosmol. Astropart. Phys. 06 (2014) 002.

[98] B. J. Kavanagh, P. Panci, and R. Ziegler, J. High Energy Phys. 04 (2019) 089.

[99] X. Chu, J. Pradler, and L. Semmelrock, Phys. Rev. D **99**, 015040 (2019).

[100] T. Banks, J.-F. Fortin, and S. Thomas, arXiv:1007.5515.

[101] J. Bagnasco, M. Dine, and S. D. Thomas, Phys. Lett. B **320**, 99 (1994).

[102] S. Chang, A. Pierce, and N. Weiner, J. Cosmol. Astropart. Phys. 01 (2010) 006.

[103] A. V. Manohar and M. B. Wise, *Heavy Quark Physics* (Cambridge University Press, Cambridge, England, 2000), Vol. 10.

[104] T. Piffl *et al.*, Astron. Astrophys. **562**, A91 (2014).

[105] G. Monari, B. Famaey, I. Carrillo, T. Piffl, M. Steinmetz, R. F. G. Wyse, F. Anders, C. Chiappini, and K. Janßen, Astron. Astrophys. **616**, L9 (2018).

[106] Y. Hochberg, M. Pyle, Y. Zhao, and K. M. Zurek, J. High Energy Phys. 08 (2016) 057.

[107] A. I. Kakhidze and I. V. Kolokolov, Sov. Phys. JETP **72**, 598 (1991).

[108] D. J. E. Marsh, K.-C. Fong, E. W. Lentz, L. Smejkal, and M. N. Ali, Phys. Rev. Lett. **123**, 121601 (2019).

[109] R. Barbieri, C. Braggio, G. Carugno, C. S. Gallo, A. Lombardi, A. Ortolan, R. Pengo, G. Ruoso, and C. C. Speake, Phys. Dark Universe **15**, 135 (2017).

[110] N. Crescini *et al.*, Eur. Phys. J. C **78**, 703 (2018); **78**, 813(E) (2018).

[111] N. Crescini *et al.* (QUAX Collaboration), Phys. Rev. Lett. **124**, 171801 (2020).